THE JOURNAL OF BIOLOGICAL CHEMISTRY
© 1989 by The American Society for Biochemistry and Molecular Biology, Inc.

Vol. 264, No. 14, Issue of May 15, pp. 8171-8178, 1989
Printed in U.S.A.

Fluorescent Indicators for Cytosolic Calcium Based on Rhodamine and Fluorescein Chromophores*

(Received for publication, December 7, 1988)

Akwasi Minta‡, Joseph P. Y. Kao, and Roger Y. Tsien§

From the Department of Physiology-Anatomy, University of California, Berkeley, California 94720

A new group of fluorescent indicators with visible excitation and emission wavelengths has been synthesized for measurements of cytosolic free Ca^{2+}. The five compounds, "rhod-1," "rhod-2," "fluo-1," "fluo-2," and "fluo-3" (Figs. 2 and 3), combine the 8-coordinate tetracarboxylate chelating site of 1,2-bis(2-aminophenoxyethane-*N*,*N*,*N*′,*N*′-tetraacetic acid with a xanthene chromophore to give a rhodamine-like or fluorescein-like fluorophore. Binding of Ca^{2+} increases the fluorescence by up to 40-fold. The Ca^{2+} dissociation constants are in the range 0.37–2.3 μM, so that the new indicators should give better resolution of high $[Ca^{2+}]$ levels than previously obtainable with quin-2 or fura-2. The visible excitation wavelengths of the new compounds are more convenient for fluorescence microscopy and flow cytometry than the UV required by previous indicators. However, the new dyes' increase in fluorescence upon binding calcium is not accompanied by a wavelength shift, so they are unsuitable for measurements using ratios at two wavelengths. The most promising dye of this series is fluo-3, whose initial biological testing in fibroblasts is described in the following paper (Kao, J. P. Y., Harootunian, A. T., and Tsien, R. Y. (1989) *J. Biol. Chem.* 264, 8171–8178).

Advances in techniques for measuring cytosolic free Ca^{2+} concentrations ($[Ca^{2+}]_i$) have been essential to our understanding of calcium as an intracellular messenger. The tetracarboxylate fluorescent indicators quin-2, fura-2, and indo-1 (1–6) are the basis for the most widely used methods for measuring $[Ca^{2+}]_i$. Their popularity stems from the ease with which they can be loaded into cells by hydrolysis of membrane-permeant esters, as well as the sensitivity and versatility of fluorescence, a mode of readout adaptable to bulk suspensions, flow cytometry, and microscopic imaging of single cells. However, the existing dyes all require excitation at ultraviolet wavelengths near the cut-off for transmission through glass. Many specialized fluorescence instruments require laser excitation, which is much more expensive to produce in the UV compared to the visible range. UV wavelengths are also potentially injurious to cells (*e.g.* Ref. 7) and tend to excite autofluorescence, for example from pyridine nucleotides. Also, the UV range coincides with that needed to photolyze chelators such as nitr-5, nitr-7, and DM-nitrophen to release their bound Ca^{2+} (8–11). Therefore, the existing indicators cannot readily be used to monitor release of "caged" Ca^{2+} because the fluorescence excitation would begin to photolyze the buffer. Moreover, the absorbance of the nitr-5 or nitr-7 and their photolysis reaction products may cause inner filtering that can artifactually perturb the fluorescence excitation. All these problems with UV could be avoided with Ca^{2+} indicators whose excitation wavelengths were in the visible or infrared range. Such dyes have long been a major goal of ours, but previous attempts have given products with disappointing fluorescence quantum efficiencies or Ca^{2+} affinities (1).

The fluorophores most widely used in biology are probably those of fluorescein and rhodamine (Fig. 1*A*). Because of their ubiquity as labels in immunofluorescence and fluorescent analog cytochemistry (12), practically all fluorescence microscopes and flow cytometers are equipped to handle their wavelengths. It was therefore of obvious interest to try to marry these highly fluorescent delocalized xanthenes to the proven Ca^{2+}-specific binding site of BAPTA.[1] One possibility would be to replace a dialkylamino group in a rhodamine or rhodol dye with a bis(carboxymethyl)amino group as in Fig. 1*B*. However, we feared that the vinylogous amide or amidine structure would withdraw too much electron density from the chelating amino nitrogen, reducing the Ca^{2+} affinity excessively and perhaps even promoting hydrolytic loss of the bis(carboxymethyl)amino group. We therefore chose instead to attach the BAPTA moiety to the central 9-position of the xanthene so that the latter would remain symmetrical. Such symmetry is desirable because nearly all long-wavelength dyes that are highly fluorescent in water have highly symmetrical polymethine chromophores, whereas asymmetrical chromophores such as merocyanines and rhodols are generally poorly fluorescent in water (14).

Classical rhodamines and fluoresceins (Fig. 1*A*) are prepared from *m*-dialkylaminophenols or resorcinols condensed with phthalic anhydrides under harsh conditions. Mixtures of isomers which are separated with difficulty are generated when the phthalic anhydride bears nonequivalent substituents as would be required for the BAPTA moiety to be attached to the 9-position. Also, an extra carboxyl would be left adjacent to the junction of the xanthene and phthalein rings. This carboxyl might be undesirable for our purposes because it would interfere sterically with the conjugation between the xanthene system and the phthalein ring. If this conjugation were reduced too much, the fluorophore might

* This work was funded by Grants GM31004 and EY04372 from the National Institutes of Health and Grant 83-K-111 from the Searle Scholars Program. The costs of publication of this article were defrayed in part by the payment of page charges. This article must therefore be hereby marked "*advertisement*" in accordance with 18 U.S.C. Section 1734 solely to indicate this fact.

‡ Present address: Molecular Probes, Inc., P.O. Box 22010, Eugene, OR 97402.

§ To whom correspondence should be addressed.

[1] The abbreviations used are: BAPTA, 1,2-bis(2-aminophenoxyethane-*N*,*N*,*N*′,*N*′-tetraacetic acid; HEEDTA, *N*-(2-hydroxyethyl)ethylenediamine-*N*,*N*′,*N*′-triacetic acid; NTA, nitrilotriacetic acid; MOPS, 3-(*N*-morpholino)propanesulfonic acid; EGTA, [ethylenebis(oxyethylenenitrilo)]tetraacetic acid.

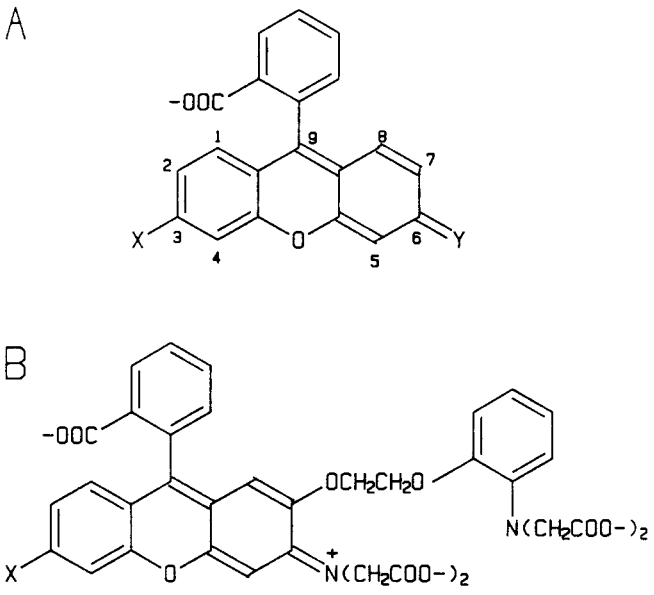

FIG. 1. *A*, structure of conventional rhodamines, rhodols, and fluoresceins. In a rhodamine, *X* would be a substituted amino group, R^1R^2N–, and *Y* would be similar but positively charged, $=N^+R^1R^2$. In a rhodol, *X* is as above, while *Y* becomes =O. In a fluorescein, *X* and *Y* are ^-O– and =O, respectively. *B*, a possible design for a Ca^{2+} indicator in which the chelating site directly includes the xanthene chromophore. *X* would be R^1R^2N– or ^-O–.

become insulated from the chelating site and no longer signal Ca^{2+} binding. Synthetic routes were therefore devised to avoid phthalic anhydrides and the generation of this extra carboxyl. The BAPTA moiety was activated either by an extra hydroxy substituent as in rhod-1 and fluo-1, or by formation of an organolithium derivative as in rhod-2, fluo-2, and fluo-3, and then coupled with various 9-xanthones.

EXPERIMENTAL PROCEDURES

The synthetic routes to the new dyes are outlined in Figs. 2 and 3. and fully described below. Proton NMR spectra were recorded on Varian EM-390 at 90 MHz, UCB 200 MHz, and Bruker AM 500 MHz spectrometers. Peaks are reported below in the following format: NMR (solvent, operating frequency): chemical shift (δ) in parts/million from tetramethysilane, multiplicity (s = singlet, d = doublet, dd = doublet of doublets, t = triplet, q = quartet, m = multiplet, br = broad), spin-spin coupling constant if appropriate, integrated number of protons; sometimes several adjacent peaks are too close for their integral to be separated, in which case only the total integral for a cluster is stated.

I—1-(2-Bis(ethoxycarbonylmethyl)amino-4-benzyloxyphenoxy)-2-(2-bis(ethoxycarbonylmethyl)amino-5-methylphenoxy)ethane, compound XXIV of Grynkiewicz *et al.* (3), 1 g, was dissolved in acetic acid (15 ml) and hydrogenated at atmospheric pressure with 5% palladium on charcoal. After complete uptake of hydrogen (overnight required), the catalyst was filtered off and the filtrate evaporated to dryness. Trituration of the product with toluene gave a cream-colored solid in nearly quantitative yield, m.p. 82–84 °C. NMR ($CDCl_3$, 90 MHz): δ 1.10, t, 12H; 2.20, s, 3H; 4.00, s + q, 16H; 4.85, s, 4H; 6.45, s, 1H; 6.60, dd, 3H; 7.30, m, 3H.

I + *II* → *III*—The phenol VI (120 mg, 0.2 mmol) was dissolved in dry chloroform (2 ml). 3,6-Dimethylaminoxanthone, prepared following Ehrlich and Benda (19) (60 mg, 0.21 mmol), converted to the chlorocarbonium ion by stirring with oxalyl chloride (18), was added in dry chloroform. After stirring at room temperature overnight, the reaction mixture was diluted with more chloroform and washed with sodium bicarbonate and then evaporated to give a pinkish purple gum. This residue was purified by chromatography on silica gel to give a pinkish purple solid (56 mg, 32%). NMR ($CDCl_3$, 90 MHz): δ 1.20, t, 12H; 2.05, s, 3H; 3.15, s, 12H; 4.00–4.30, 2s + q, 20H; 6.25, s, br, 1H; 6.50–6.80, m, 8H; 7.20, d, 12 Hz, 1H; 7.60, d, 12Hz, 1H.

III → *rhod-1*—The ester XIV (4 mg) was dissolved in methanol (500 μl). Dioxane (200 μl) and aqueous KOH (1 M, 200 μl) were added. The reaction mixture was stirred at room temperature and monitored by thin layer chromatography until all the ester had hydrolyzed. The reaction mixture was then evaporated to dryness and redissolved in water. Acidification to pH 2 gave a dark purplish solid (rhod-1).

I + *IV* → *V* → *fluo-1*—The phenol I (40 mg, 0.06 mmol) and 3,6-di(benzyloxy)xanthone (IV, prepared by benzylation of 3,6-dihydroxy-9-xanthone (20)) were dissolved in $POCl_3$ and heated at 100 °C for 2 h. The reaction mixture containing V was evaporated *in vacuo*, taken into acetic acid, and a little formic acid was added. The mixture was heated under reflux overnight to remove the protecting groups and evaporated *in vacuo*. The residue was taken into basic buffer and washed with ethyl acetate three times. Acidification with hydrochloric acid to pH 2 gave fluo-1 as a reddish brown solid.

VI—1-(2-Aminophenoxy)-2-(2-amino-5-methylphenoxy)ethane, compound V of Grynkiewicz *et al.* (3) (1.032 g, 4 mmol), 1,8-bis(dimethylamino)naphthalene (4.4 g, 20 mmol), anhydrous sodium iodide (200 mg, 1.2 mmol), *tert*-butyl bromoacetate (4.680 g, 24 mmol), and acetonitrile (10 ml) were stirred with heating under reflux for 18 h. The cooled mixture was diluted with toluene and filtered. The filtrate was extracted with phosphate buffer at pH 2 until the 1,8-bis(dimethylamino)naphthalene was removed. The toluene solution was then dried and evaporated to dryness. The residue crystallized from ethanol gave white needles (2.4 g, 86% yield), m.p. 118–119.5 °C. NMR ($CDCl_3$, 90 MHz): δ 1.40, s, 36H; 2.25, s, 3H; 4.00, s, 4H, 4.05, s, 4H; 4.30, s, 4H; 6.85, m, 3H; 6.90, s, 4H.

VI → *VII*—The ester VI (2.16 g, 3 mmol) was dissolved in 30 ml of dichloromethane and cooled to −78 °C. Pyridine (355 mg, 4.5 mmol) was added and the mixture was stirred while bromine (572 mg, 3.6 mmol) in dichloromethane (5 ml) was added. The mixture was allowed to warm up to room temperature and then evaporated *in vacuo*. The residue was taken into chloroform and washed with water, sodium bicarbonate solution, and then brine. The organic layer was dried and the residue crystallized with ethanol (2.01 g, 83%), m.p. 129–131 °C. NMR ($CDCl_3$, 90 MHz): δ 1.42, s, 36H; 2.25, s, 3H; 4.00, s, 8H; 4.35, s, 4H; 6.75, d + m, 3H; 6.85–7.05, s + m, 3H.

VII → *VIII*; *VIII* + *II* → *IX*—The bromide VII (80 mg, 0.1 mmol) was dissolved in 2-methyltetrahydrofuran (2 ml) and stirred at −150 °C in a liquid nitrogen/isopentane bath. Tertiary butyllithium (6 equivalents) in hexane (1.7 M, Aldrich) was added and the metallation monitored by thin layer chromatography of small samples quenched into water. When metallation was complete, the samples showed only the dehalogenated ester VI instead of the bromo compound VII. 3,6-Bis(dimethylamino)xanth-9-one (II) (43 mg, 0.15 mmol) (19) dissolved in tetrahydrofuran was added dropwise to the reaction mixture. Stirring was continued for another 30 min; the bath temperature was not allowed to rise above −130 °C. The reaction mixture was quenched with water in tetrahydrofuran and then allowed to warm up to room temperature. It was then extracted twice with ethyl acetate. The combined organic extracts were backwashed with brine and evaporated to dryness. The residue was then stirred with acetic acid to convert all the leuco base into the dye. Evaporation of the acetic acid *in vacuo* left a gummy residue which was purified by column chromatography on silica gel (25 mg, 25% yield). NMR ($CDCl_3$, 500 MHz): δ 1.38, s, 18H; 1.50, s, 18H; 2.30, s, 3H; 3.35, s, 12H; 3.90, s, 4H; 4.20, s, 4H; 4.40, s, 4H; 6.70–6.90, m, 9H; 7.55, d, 1H; 8.15, d, 1H.

IX → *rhod-2*—The ester IX (4 mg) was dissolved in acetic acid (500 μl) and BF_3 etherate (50 μl) was added. The resulting solution was stirred at room temperature overnight. The solution was then evaporated *in vacuo* at 35 °C and then basified with buffer. The basic solution was washed three times with ethyl acetate and then acidified with hydrochloric acid to pH 2 to give rhod-2 as a dark purplish solid.

X—3,6-Dihydroxyxanth-9-one (20), 115 mg, 0.5 mmol, was dissolved in dry dimethylformamide. Imidazole (340 mg, 5 mmol) and *t*-butyldimethylchlorosilane (450 mg, 3 mmol) were added. After stirring at room temperature for 2 h, the mixture was diluted with toluene, washed extensively with water and dried over $MgSO_4$. Evaporation *in vacuo* gave a white solid, which was recrystallized from ethanol to give 185 mg (77%) of white needles, m.p. 151–154 °C. NMR ($CDCl_3$, 90 MHz): δ 0.20, s, 12H; 0.90, s, 18H; 6.80, m, 4H; 8.15, d, 9Hz, 2H.

VIII + *X* → *XI*—The bromide VII (80 mg, 0.1 mmol) was converted to organolithium intermediate VIII and reacted with X, 3,6-bis(*t*-butyldimethylsilyloxy)xanthone (100 mg, 0.20 mmol) in analogy to the preparation of IX described above. The ester XI was obtained as a reddish brown solid (45 mg, 48%). NMR ($CDCl_3$, 500 MHz): δ 1.40, s, 18H; 1.50, s, 18H; 2.30, s, 3H; 3.98, s, 4H; 4.20, s, 4H; 4.37, s, 4H; 6.70, d + s, 2H; 6.95, m, 9H; 7.40, d, 1H.

XI → fluo-2—The *t*-butyl groups in XI (5 mg) were removed with BF_3 etherate in acetic acid just as in the preparation of rhod-2 above, giving fluo-2 as a reddish brown solid.

XII—2,7-Dichloro-3,6-dihydroxyxanth-9-one (450 mg, 1.5 mmol), obtained following Kurduker and Subba Rao (22), was derivatized with imidazole (1.02 g, 15 mmol) and *t*-butyldimethylchlorosilane (1.35 g, 9 mmol) in dimethylformamide just as described for X above. The bis(*t*-butyldimethylsilyl) ether XII was recrystallized from ethanol to give 660 mg (78%) white needles, m.p. 161–164 °C. NMR ($CDCl_3$, 90 MHz): δ 0.15, s, 12H; 0.95, s, 18H; 6.20, s, 2H; 7.35, s, 2H.

VIII + XII → XIII—The bromide II (80 mg, 0.1 mmol) was converted to the organolithium derivative VIII, reacted with XII (90 mg, 0.17 mmol), and worked up as described above for the preparation of IX. XIII was obtained as a red solid (55 mg, 55% yield). It was further purified by centrifugal chromatography in silica eluted with hexane/ethyl acetate/acetic acid (50:50:1, v/v) followed by crystallization from diisopropyl ether, m.p. 188–192 °C, with decomposition. NMR ($CDCl_3$, 200 MHz): δ 1.40, s, 18H; 1.50, s, 18H; 2.30, s, 3H; 3.85, s, 4H; 4.05, s, 4H; 4.42, s, 4H; 7.35, s, 1H; 6.75–7.20, m, 9H. The visible spectrum in ethanol solution containing a trace of triethylamine showed a main peak at 520 nm ($\epsilon = 1.02 \times 10^5$ M^{-1} cm^{-1}) with a shoulder at 486 nm ($\epsilon = 2.91 \times 10^4$).

XIII → fluo-3—The *t*-butyl groups in ester XIII (2 mg) were removed with BF_3 etherate in acetic acid as described already for rhod-2. Fluo-3 was obtained as a reddish brown solid. For determination of the extinction coefficient, the number of micromoles of dye was based on the weight of the starting ester XIII rather than of the free acid, which contained some inert residues from the de-esterification reagents.

Preparation of Acetoxymethyl Esters—Free acids were esterified with acetoxymethyl bromide by standard means (3).

Optical spectra of the free chelators were measured as described previously (3). Quantum efficiencies of fluorescence were obtained (15) by comparing the integral of the corrected emission spectrum of the test sample with that of a solution of rhodamine B in ethanol, quantum efficiency assumed to be 0.97 (16), or fluorescein in 0.1 M NaOH, quantum efficiency 0.91 (15). The concentration of the reference dye was adjusted to match the absorbance of the test sample at the wavelength of excitation.

For measurement of Ca^{2+} dissociation constants at pH 7.0–7.5, free [Ca^{2+}] levels were controlled by Ca^{2+}·EGTA, Ca^{2+}·HEEDTA, and Ca^{2+}·NTA buffers (17). The apparent dissociation constant for the Ca^{2+}·EGTA complex was taken as 327 nM at pH 7.03 in 100 mM KCl, 20 °C. The logarithms of the apparent dissociation constants for the Ca^{2+}·HEEDTA and Ca^{2+}·NTA complexes were calculated to be 1.70 − pH and 3.41 − pH, respectively, at room temperature in 0.1 M KCl. To test the pH dependence of the apparent Ca^{2+} dissociation constant of fluo-3 (Fig. 4), it was necessary to vary pH from 5.6 to 8 while maintaining constant free Ca^{2+}. EGTA, HEEDTA, and NTA are too pH-dependent to cover this pH range, so dibromo-BAPTA (chelator 2c of Ref. 13) was used instead. Because the highest pK_a of this chelator is 5.6, the effective Ca^{2+} affinity is only slightly pH-dependent from pH 5.6 upwards. To compensate for that small dependence, the pH titration was started from pH 5.6 with the appropriate amount of Ca^{2+} in the buffer. Then at each higher pH, the appropriate small addition of $CaCl_2$ was made to compensate for the increase in the effective Ca^{2+} affinity of the dibromo-BAPTA.

Free [Mg^{2+}] was controlled by Mg^{2+}·EGTA buffers assuming an apparent dissociation constant for the Mg^{2+}·EGTA complex (including its monoprotonated form) of 6 mM at pH 7.60, 0.12 M ionic strength, 20 °C as calculated from the data of Martell and Smith (17).

The Mn^{2+}:Ca^{2+} and Zn^{2+}:Ca^{2+} selectivities of fluo-3 were determined as in Ref. 3 by fluorescence titrations of 2 μM fluo-3 with 0–20 mM Ca^{2+} in the presence of 40 μM Mn^{2+} or 20 μM Zn^{2+}. Also, 2 μM fluo-3 in 8 or 20 mM Ca^{2+} was titrated with 0–8 mM Mn^{2+} or 0–2 mM Zn^{2+}.

RESULTS

Organic Syntheses—Two key intermediates and two distinct routes were employed in the syntheses of these compounds. The first route (Fig. 2) was based on I, a BAPTA derivative with an extra hydroxyl group *meta* to the tertiary amino group on one ring, prepared by debenzylation of compound XXIV of Grynkiewicz *et al.* (3). The added phenolic-OH activated the ring sufficiently to permit electrophilic substitution by a 9-xanthone (II or IV), itself activated (18) by $(COCl)_2$ or $POCl_3$. 3,6-Dimethylaminoxanthone (II), prepared following Ref. 19, gave after saponification a rhodamine analog, rhod-1, while 3,6-dihydroxyxanthone (20) with the hydroxy groups protected as benzyl ethers (IV) gave a fluorescein analog, fluo-1. Attempts to couple xanthones with BAPTA lacking the extra phenolic-OH failed. The second route (Fig. 3) was therefore devised to provide an alternative and stronger form of activation of the BAPTA nucleus via an organolithium intermediate. Though organolithium reagents normally attack nearly all protected forms of carboxylates, we found in agreement with Parham (21) that *t*-butyl esters were resistant enough below −150 °C to allow lithium-bromine exchange. The lithiation required six equivalents of tertiary butyllithium (*t*-BuLi) to go to completion, four of which were presumably used to enolize the four ester carbonyls, one to supply the lithium going onto the aryl ring, and one to destroy the *t*-butyl bromide formed. Once formed, the *p*-lithio-BAPTA (VIII) was treated *in situ* with 3,6-bis(dimethylamino)xanthone (II) to give rhod-2, or with 3,6-dihydroxyxanthone (X, protected with *t*-butyldimethylsilyl groups) to give the fluorescein analog fluo-2, or with 2,7-dichloro-3,6-dihydroxyxanthone (22) (XII, likewise protected) to give fluo-3. The free dyes were obtained by removing the protecting groups with boron trifluoride in acetic acid.

Absorbance and Fluorescence Properties—The absorbance and fluorescence properties for the new indicators in the presence and absence of Ca^{2+} are compiled in Table I. The absorbance spectra were much as one would expect for rhodamine or fluorescein chromophores, although extinction coefficients (not shown) were often low in the dyes as initially isolated. Because fluo-3 proved to be the most promising candidate, extra effort was expended in its purification. Eventually, quite respectable extinction coefficients were obtained, 7.9×10^4 and 8.3×10^4 M^{-1} cm^{-1} at 503 and 506 nm, respectively, for free and Ca^{2+}-bound fluo-3. Ca^{2+} binding was expected to shift the absorbance maxima to longer wavelengths, since it would prevent the BAPTA amino nitrogen from donating electron density to the 9-position of the xanthene. Electron withdrawal and donation to the central carbon of triphenylmethane dyes are known to shift absorbance peaks to longer and shorter wavelengths, respectively (23). Indeed Ca^{2+} binding caused red shifts, but of very small magnitude, 1–3 nm, and with little change in peak height.

All the compounds showed fluorescence qualitatively similar to rhodamines or fluoresceins as expected. For example, Fig. 4 shows excitation and emission spectra for fluo-3 as a function of free [Ca^{2+}] in EGTA buffers. Fluo-3 has a visibly pinkish tinge because its chlorine atoms shift its spectra to wavelengths slightly longer than those of fluo-2, just as 2,7-dichlorofluorescein is bathochromically shifted from fluorescein. Fluorescence intensities were very strongly enhanced by Ca^{2+} binding. Thus, the Ca^{2+} complex of fluo-3 fluoresced 35–40-fold more brightly than the Ca^{2+}-free dye (Fig. 4). This degree of enhancement is the greatest yet reported for a fluorescent Ca^{2+} indicator. However, Ca^{2+} binding caused little change in the wavelengths of peak excitation or emission, so that these dyes gave no useful change in excitation or emission ratio. Also, even with Ca^{2+} bound, the quantum efficiencies of fluorescence were considerably less than those of true rhodamines or fluoresceins in water (up to 0.9), though comparable with those of model compounds such as 9-phenylfluorone, quantum efficiency 0.21 (24), that similarly lack the extra phthalein carboxyl.

Fluo-3 was briefly checked for photochemical stability. In air-saturated solutions illuminated with a xenon arc filtered only by glass lenses, Ca^{2+}-free fluo-3 bleached at about the

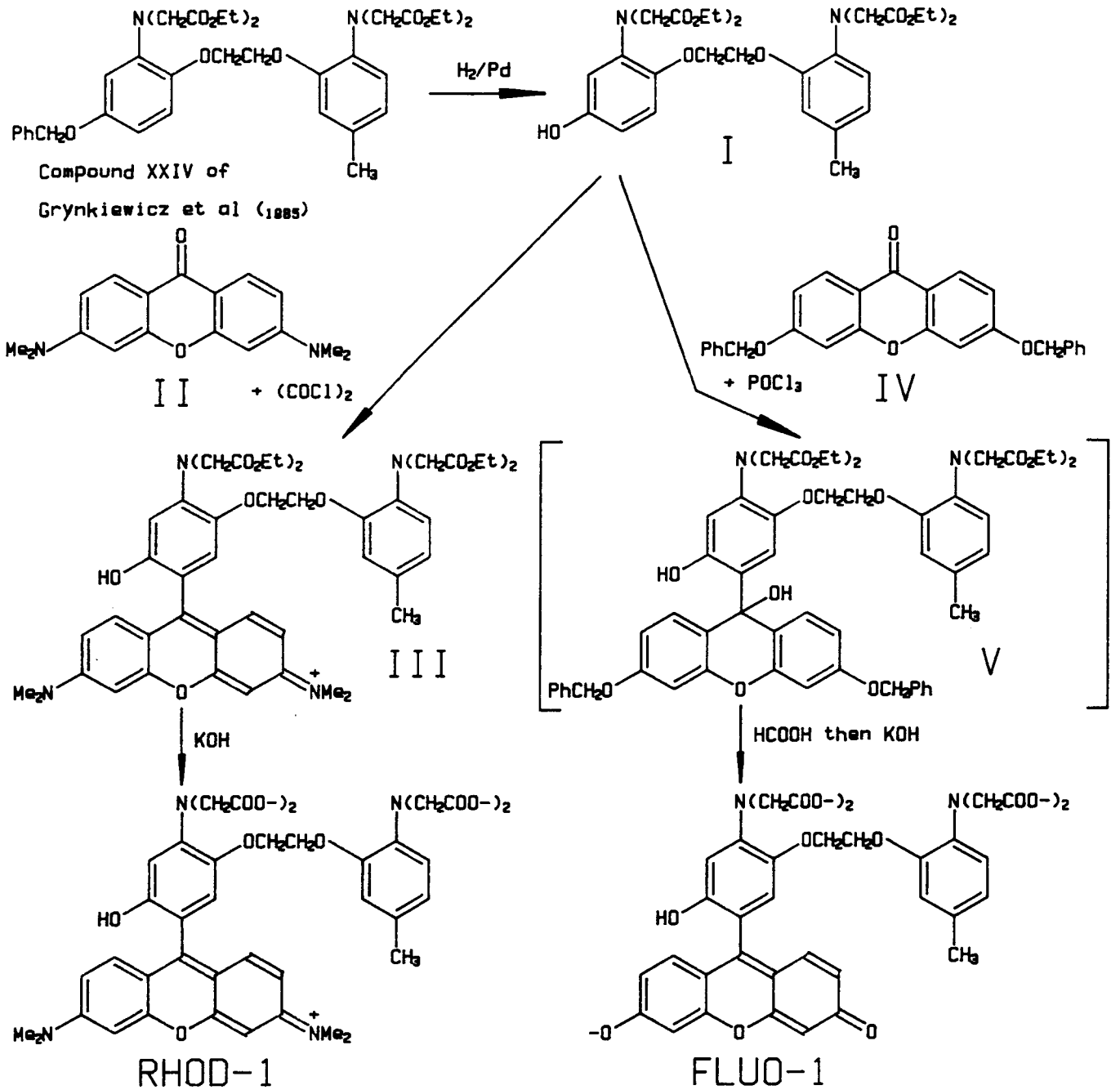

FIG. 2. **Synthetic pathway leading to rhod-1 and fluo-1.** *Roman numerals* are keyed to the synthetic details under "Experimental Procedures." Structures in *brackets* were used *in situ* without isolation.

same rate as ordinary fluorescein anion, whereas the Ca^{2+} complex bleached about half as quickly. Since the biological usability of fluorescein is well established, the photochemical resistance of fluo-3 would seem to be adequate if not outstanding.

Ca^{2+}-binding Constants—Ca^{2+} dissociation constants for all the new chelators (Table I) are in the range 370 nM to 2.3 μM at ionic strengths 0.1–0.15. These values are significantly higher than those for the parent compounds BAPTA (110 nM, Ref. 13) and its *p*-methyl derivative "benz4" (79 nM, Ref. 10), indicating that the xanthene chromophores are somewhat electron-withdrawing. The positively charged rhodamines are distinctly lower in affinity than the negatively charged fluoresceins, as expected. A hydroxy group on the BAPTA aromatic ring as in rhod-1 and fluo-1 also lowers the Ca^{2+} affinity more than twofold compared to the unsubstituted rhod-2 and fluo-2, presumably because a hydroxy group is inductively electron withdrawing when *meta* to the reaction center, the amino nitrogen. The chlorines added in fluo-3 have very little effect, because they are too far from the chelating site.

Cation Selectivity—The fluoresceins fluo-1 and fluo-2 were expected and found to show some pH dependence due to the ability of the phenolic hydroxyl on the xanthene chromophore to accept a proton. For example, the fluorescence of fluo-2 was almost completely quenched as the pH was titrated from pH 7.7 to 4.1 in the absence of Ca^{2+}. The titration curve fitted a pK_a of 6.20 ± 0.02 and a ratio of 67 between the fluorescence brightness of the deprotonated and the protonated species. Because protonation quenches fluorescence, this pK_a is probably on the fluorescein chromophore not the chelator amino group. Protonation of the latter would be expected to act like Ca^{2+} and enhance fluorescence. A pK_a of 6.2 would normally

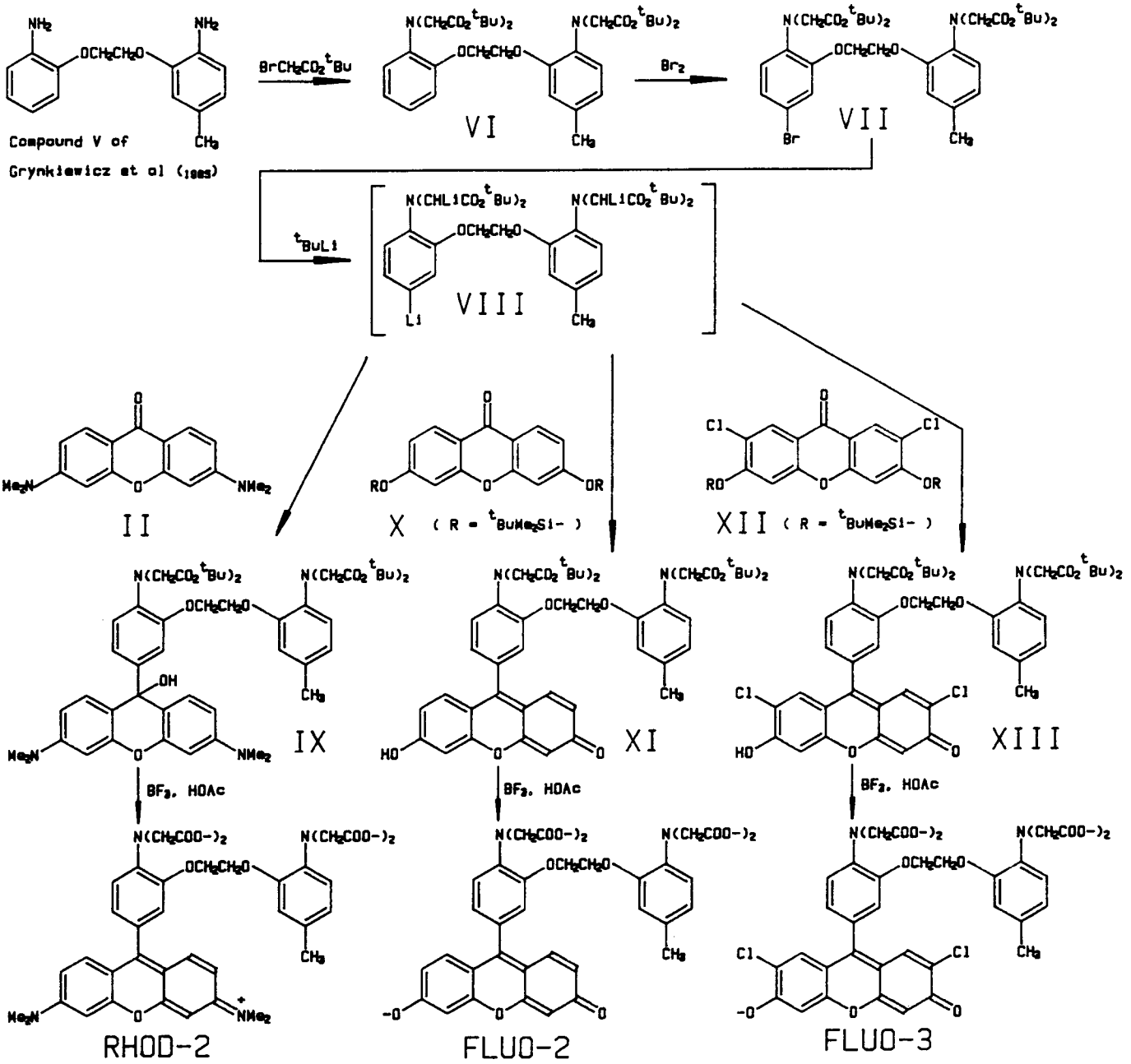

FIG. 3. **Synthetic pathway leading to rhod-2, fluo-2, and fluo-3.**

be fairly safely remote from typical cytosolic pH values, but because protonation has such a powerful effect on the fluorescence and is spectrally indistinguishable from a drop in $[Ca^{2+}]$, fluo-2 is too pH-sensitive for general use. This problem was the motivation for the synthesis of fluo-3 with chloro substituents to increase the acidity of the chromophore. The pK_a fell to 4.5–4.6 as assessed either by the absorbance spectrum, which was practically Ca^{2+}-independent, or by the fluorescence amplitude of the Ca^{2+}-complex at saturating (millimolar) Ca^{2+} levels (*top curve*, Fig. 5). Because this pK_a was shifted to such a low value, it became possible to detect protonation on an amino nitrogen with a pK_a of about 6.2. This protonation was revealed by a modest increase, maximally 3-fold, of the fluorescence of the Ca^{2+}-free dye as the pH was titrated from pH 8 to 5 (*bottom curve*, Fig. 5). Amino protonation is similar to Ca^{2+} binding in that both have negligible effect on the absorbance spectrum yet enhance fluorescence quantum efficiency. Protonation tends to inhibit Ca^{2+} binding, as shown by the two curves at intermediate $[Ca^{2+}]$ in Fig. 5. At pH ~6.1–6.2, a given intermediate concentration of Ca^{2+} is about half as effective at enhancing fluorescence as it is at pH ~8, an independent rough confirmation of an amino pK_a near 6.2.

The Mg^{2+} dissociation constant for fluo-3 was found to be 9 mM at 25 °C, 0.1–0.15 M ionic strength. This value is practically the same as that (8.1 mM, Ref. 10) of the parent compound benz4 lacking the xanthene chromophore. Evidently the electron-withdrawing effect of the xanthene does not affect the Mg^{2+} affinity nearly as much as it reduces the Ca^{2+} affinity. This result can be explained if the Mg^{2+} binds mainly to the half of the chelator that is remote from the chromophore. In confirmation of this hypothesis, Mg^{2+} binding also has relatively little effect on the chelator fluorescence, boosting it only about 1.4 fold, much less than the 40-fold enhancement from Ca^{2+} binding.

Fluo-3 was also tested against manganese and zinc, the two

TABLE I

Fluorescence properties and dissociation constants of chelators based on rhodamines and fluoresceins

All data were obtained at 22 ± 2 °C in 0.1 M KCl, pH 7.0–7.5, air-equilibrated. Fluorescence excitation curves were corrected by a rhodamine B counter, but emission maxima refer to uncorrected spectra. However, because of the sharpness of the emission peaks, correction makes little difference to peak position. Quantum efficiencies and effective dissociation constants were measured as described under "Experimental Procedures;" zero Ca^{2+} refers to solutions with no added Ca^{2+} and 1–10 mM EDTA or EGTA, whereas excess Ca^{2+} solutions had 1–2 mM Ca^{2+}. For fluo-3, the fluorescence ratio of 36 refers to the ratio of quantum efficiencies, whereas a ratio of up to 40 can be obtained by setting the excitation and emission wavelengths to the peaks for the Ca^{2+} complex, which are slightly red-shifted from the free dye.

Dye	Fluorescence maxima with excess Ca^{2+}		Quantum efficiencies		Fluorescence ratio, excess *vs.* zero Ca^{2+}	Effective K_d for Ca^{2+}
	Excitation	Emission	Zero Ca^{2+}	Excess Ca^{2+}		
	nm					*μM*
rhod-1	556	578	0.0014	0.021	15	2.3
fluo-1	499	521	0.0042	0.014	3.3	0.7
rhod-2	553	576	0.03	0.102	3.4	1.0
fluo-2	493	518	0.004	0.125	31	0.37
fluo-3	506	526	0.0051	0.183	36–40	0.40

transition metals known to be able to interact with tetracarboxylate chelators inside cells (3, 25, 26). Mn^{2+} bound to fluo-3 about 70-fold as strongly as Ca^{2+} did, corresponding to a K_d for Mn^{2+} of 6.4 nM. Interestingly, the Mn^{2+} complex was about eight times as fluorescent as the metal-free dye, though only one-fifth as fluorescent as the Ca^{2+} complex. The intermediate fluorescence level of the Mn^{2+} complex is equivalent to the effect of about 100 nM free [Ca^{2+}] on fluo-3, and contrasts with the negligible fluorescence of the Mn^{2+} complexes of quin-2 and fura-2.

Zn^{2+} bound to fluo-3 approximately 300-fold more strongly than Ca^{2+} did, corresponding to a K_d for Zn^{2+} of about 1.5 nM. The Zn^{2+} complex was 61% as fluorescent as the Ca^{2+} complex, so that saturation with Zn^{2+} simulated 680 nM free [Ca^{2+}].

DISCUSSION

The most obvious difference between the present chelators and the previous tetracarboxylate Ca^{2+} chelators is in their wavelengths of fluorescence excitation and emission. The new indicators' similarity to fluoresceins and rhodamines make them optically compatible with almost any fluorometer, fluorescence microscope, or flow cytometer already used for immunofluorescence detection. The fluorescein analogs fluo-1, -2, and -3 can be excited by incandescent illumination or the prominent 488-nm line of an argon-ion laser. The rhodamine analogs rhod-1 and rhod-2 are suited to incandescent illumination, the 531-nm line of a krypton-ion laser, or the 546-nm line of a mercury arc. By contrast, the earlier dyes quin-2 and fura-2 are best excited at 340–350 or 380–390 nm from a xenon lamp. Indo-1 does best with 350–360 nm from a xenon arc or the low power UV lines of argon or krypton lasers. Optical elements for these UV wavelengths are preferably reflective or are made from quartz, glass with enhanced UV transmission, or very thin ordinary glass. Plastics or thick (>1 mm) ordinary glass elements generally give too much absorbance or autofluorescence or both. By contrast, even these cheap optical materials are compatible with blue or green excitation. Visible wavelengths make beam alignment easier, are essential for the current generation of confocal microscopes (*e.g.* Ref. 27), are less likely to excite significant

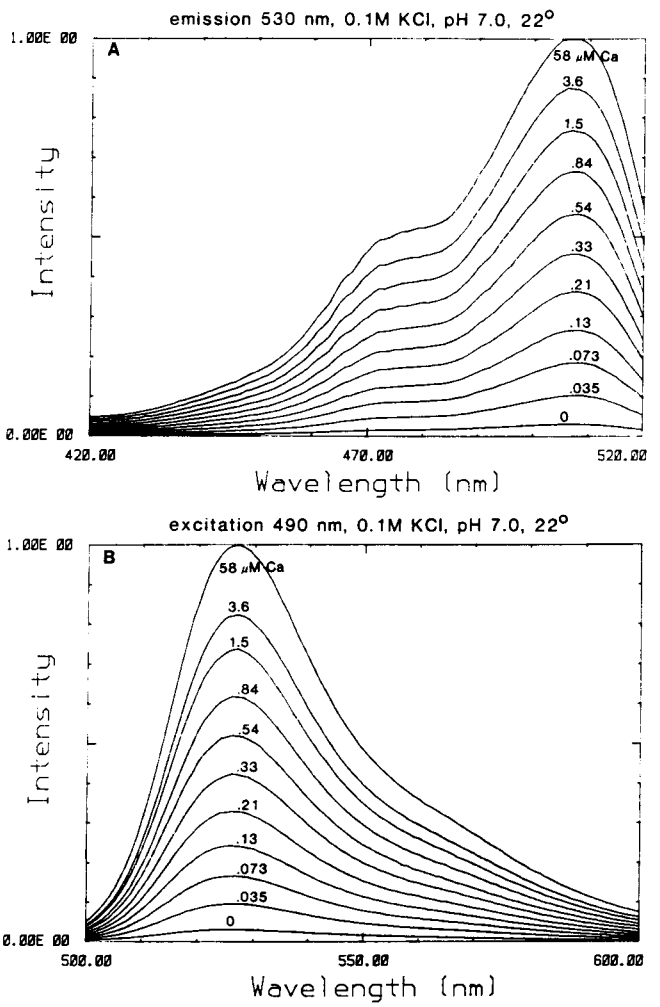

FIG. 4. **Excitation (*A*) and emission (*B*) spectra for fluo-3 at 22 ± 2 °C in buffers with free Ca^{2+} values ranging from <1 nM to 58 μM.** The titration was done starting with 3.5 ml of 100 mM KCl, 10 mM K-MOPS, 10 mM K_2H_2EGTA, 15 μM fluo-3, pH 7.03. The 0 Ca^{2+} spectrum was recorded, and then to reach n mM CaEGTA, $(10 - n)$ mM EGTA, n = 1–10, aliquots of $3.5/(11 - n)$ ml were iteratively discarded and replaced by equal volumes of 100 mM KCl, 10 mM K-MOPS, 10 mM $K_2CaEGTA$, 15 μM fluo-3, pH 7.0. After each iteration the pH (range 6.99–7.05) and spectra were recorded; each spectrum is labeled by the calculated free Ca^{2+} in micromolar. The excitation and emission bandwidths were 1.9 and 4.6 nm, respectively. All spectra have been normalized with respect to the peak of the 58 μM (n = 10) curve. *A*, emission was collected at 530 nm, and the excitation was corrected for lamp and monochromator characteristics using a rhodamine B quantum counter. *B*, excitation was at 490 nm, and the emission spectrum is uncorrected for monochromator and detector sensitivity. The slightly low amplitude of the curve at 3.6 μM [Ca^{2+}] is probably due to a small error in resetting the excitation monochromator to 490 nm.

tissue autofluorescence or to damage cells, and do not photolyze caged nucleotides or caged calcium. Therefore, the new dyes are able to quantify the [Ca^{2+}] increases produced by UV photolysis of nitr-5 or caged inositol trisphosphate (see Ref. 28, the following paper), whereas with fura-2 the excitation wavelengths began to photolyze the caged calcium and were vulnerable to inner filtering due to the high UV absorbance of the photolysis end product.[2]

Whereas fura-2 and indo-1 were clearly much more intensely fluorescent than quin-2, enabling measurements with much less added dye and Ca^{2+} buffering, comparison of the

[2] J. Kao and R. Y. Tsien, unpublished results.

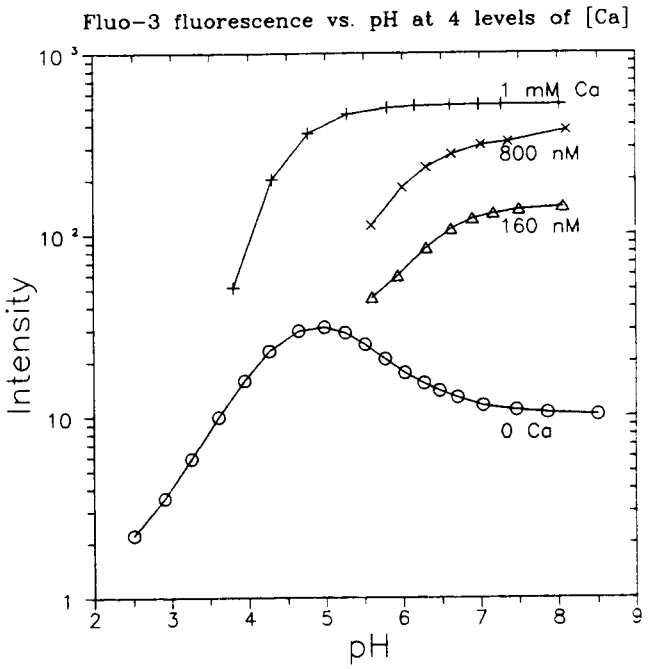

FIG. 5. **Fluorescence intensity of fluo-3 (note log axis) *versus* pH at 0, 160 nM, 800 nM, and 1 mM [Ca^{2+}], 22 ± 2 °C.** All solutions contained 10 μM fluo-3, 100 mM KCl and 10 mM Tris-MOPS and were adjusted in pH with sufficiently concentrated H_3PO_4, HOAc, or KOH so as not to change the volume significantly during the titration. The *0 Ca* points (○) were obtained with 5 mM EDTA and no added Ca^{2+}; the *160 nM* (△) and *800 nM* (×) data were obtained with 5.2 mM dibromo-BAPTA. As explained under "Experimental Procedures," the total Ca^{2+} was increased from 0.25 to 0.47 mM to maintain free [Ca^{2+}] at 160 nM as the pH was increased from 5.6 to 8.1; for 800 nM free [Ca^{2+}], total Ca^{2+} was 1.04 to 1.73 mM over the same pH range. The *1 mM Ca* (+) points were obtained with 1 mM $CaCl_2$ and no phosphate (to avoid precipitation). The ordinate in arbitrary intensity units refers to the integral of the excitation spectrum from 420 to 520 nm with emission collected at 530 nm, 9 nm band width. Because the spectra retained the same shape throughout the titration, integration was a convenient way of averaging and reducing each spectrum to a single intensity value.

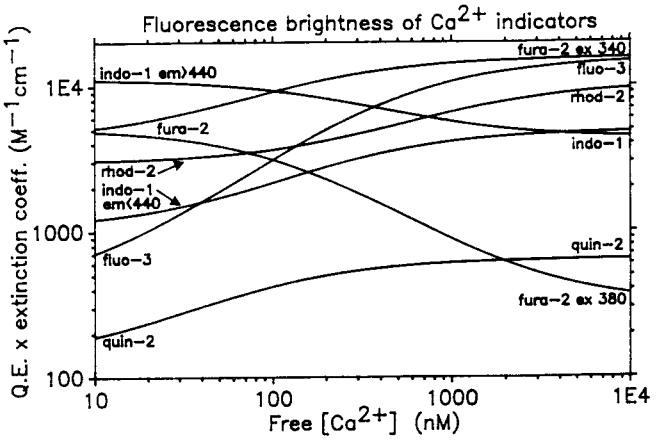

FIG. 6. **The product of fluorescence quantum efficiency (*Q.E.*) and extinction coefficient *versus* free [Ca^{2+}] (note log axes for both) for quin-2, fura-2, indo-1, rhod-2, and fluo-3.** All data are for room temperature, 0.1 M KCl, no added Mg^{2+}. The quin-2 curve was calculated for 339 nm excitation ($\epsilon = 4.6 \times 10^3$ M^{-1} cm^{-1} independent of Ca^{2+}) and quantum efficiency ranging from 0.029 to 0.14 with a Ca^{2+} dissociation constant (K_d) of 78 nM (13). The *fura-2 ex 340* curve was calculated for 340 nm excitation ($\epsilon = 1.91 \times 10^4$ to 3.19×10^4) and quantum efficiency of 0.23–0.49 with a K_d of 135 nM (3); the *fura-2 ex 380* curve was the same except based on $\epsilon = 2.25 \times 10^4$ to 6.25×10^2 for 380 nm excitation. Because indo-1 is usually employed for its emission rather than excitation shift, its curves were calculated for fixed 356 nm excitation ($\epsilon = 3.25 \times 10^4$ to 1.63×10^4) and K_d = 250 nM (3) but with the quantum efficiency (0.38–0.56) partitioned into emission components below 440 nm (0.033–0.30), and above 440 nm (0.347–0.26) for the two separate curves. The curve for fluo-3 used the data of Table I with extinction coefficients of 7.5×10^4 to 8.35×10^4 at 506 nm; the curve for rhod-2 assumed a Ca^{2+}-independent extinction coefficient of 1×10^5 M^{-1} cm^{-1}.

brightness of the new dyes with that of fura-2 and indo-1 is more complex because of the different operating wavelengths. The simplest measure of the intrinsic brightness of a fluorophore is the product of its emission quantum efficiency and its extinction coefficient at the appropriate excitation wavelength (Fig. 6). Extinction coefficients are known only for fluo-3, though one may estimate the values for the other indicators from purified model xanthene dyes ($9–10 \times 10^4$ M^{-1} cm^{-1}). For fluo-3 the quantum efficiency × extinction coefficient ranges from 3×10^3 to 1.5×10^4 M^{-1} cm^{-1} for Ca^{2+} values from 10^{-7} M up to saturation, slightly less than the corresponding values for fura-2 excited at 340 nm, 5×10^3 to 1.6×10^4 M^{-1} cm^{-1} (Fig. 6). However, it is easier to generate higher excitation intensities at longer wavelengths, and autofluorescence will be lower, so the actual concentrations of dye needed to overcome dark current and autofluorescence may be fairly similar for the two families. On the other hand, the relatively small separation between excitation and emission peaks of the new dyes makes more stringent demands on monochromators and filters to exclude scattered light.

The Ca^{2+} affinities of the new dyes are two to tenfold weaker than those of their UV-excited predecessors. This decrease improves resolution of micromolar and higher levels of $[Ca^{2+}]_i$, surprisingly without sacrificing resolution of low $[Ca^{2+}]_i$ values, at which the large change in fluorescence upon binding Ca^{2+} makes up for the decrease in percentage bound. Thus, for fluo-3, just 11 nM [Ca^{2+}] gives double the fluorescence at zero [Ca^{2+}], due to 2.5% conversion to a Ca^{2+} complex that is 40-fold brighter than the free dye. Fig. 6, which compares curves of normalized intensity *versus* log [Ca^{2+}] for fluo-3, rhod-2, quin-2, fura-2, and indo-1, emphasizes the ability of fluo-3 to respond sensitively to both low and high [Ca^{2+}] values.

The most disappointing feature of the new dyes is the small or negligible shift of absorbance, excitation, or emission wavelengths upon Ca^{2+} binding. We had hoped that Ca^{2+} binding would cause a bathochromic shift by removing electron density previously in conjugation with the 9-position of the xanthene chromophore. Numerous di- and triphenylmethane dyes and bridged heterocyclic analogs are known to show blue and red shifts, respectively, upon electron donation and withdrawal from the corresponding positions in their chromophores (23). One obvious way to rationalize the lack of shift in the present dyes is to postulate severe steric hindrance between the rigidly planar xanthene chromophore and the benzene ring of BAPTA. If the two systems were twisted out of coplanarity, Ca^{2+} binding and immobilization of the lone pair on the amino group would be insulated from the xanthene. Then why does Ca^{2+} binding affect the quantum efficiency so dramatically? Perhaps if the amino group is free, the excited state includes a significant contribution from a resonance form with increased bond orders from amino nitrogen to benzene ring and from that to the xanthene. Such increased double-bond character would demand coplanarity, which would conflict with the steric hindrance and result in radiationless deactivation.

Because Ca^{2+} hardly shifts the new dyes' wavelengths, there are no wavelength pairs in either excitation or emission

suitable for fluorescence ratioing. Ratioing is extremely valuable with single cells because it cancels out variations in dye concentration and path length. Without ratioing, one cannot convert intensity into Ca^{2+} levels unless the dye concentration, path length, and instrumental sensitivity are either 1) precisely known or 2) can be held constant while the dye is titrated to known $[Ca^{2+}]$ values. The first condition is readily satisfied in extracellular medium in a cuvet, or with somewhat greater difficulty in cells that can be internally perfused with known dye concentrations and whose dimensions can be measured microscopically. The second option can be achieved in suspensions of disaggregated cells by lysing the cells and titrating the supernatant. The alternative of using a Ca^{2+} ionophore to raise $[Ca^{2+}]_i$ to saturate the dye without lysis is made more difficult by the weakening of the Ca^{2+} affinity. Therefore, estimation of absolute $[Ca^{2+}]_i$ in nonperfused single cells is likely to be more difficult with the new dyes than with fura-2 or indo-1. However, if one is content with just a qualitative uncalibrated index of $[Ca^{2+}]_i$ changes, the new dyes are highly sensitive (Fig. 6) without the complexity of alternating wavelengths.

Ratioing is so attractive for single cells and monolayers that one must consider three alternative means of generating ratios. One method would be simultaneously to introduce a separate Ca^{2+}-independent dye working at different wavelengths. This strategem is analogous to the method of Geisow (29) to assess endosomal pH by the ratio of the signals from pH-dependent fluorescein-dextran conjugates and pH-independent rhodamine-dextran simultaneously presented for endocytosis. It is important to insure a constant ratio between the uptake of the two indicators, a reproducibility that may be difficult to achieve on a cell-to-cell basis unless both fluorophores are trace labels on similar macromolecules. Any differential leakage, compartmentation, bleaching, or metabolism would further jeopardize the fluorescence ratio as a measure of $[Ca^{2+}]_i$. Covalent linkage of the two fluorophores to each other would rule out the first two but not the latter two modes of degradation.

An alternative mode of ratioing is over time rather than over two wavelengths, so that fluorescences during cell stimulation or other manipulation are ratioed against pretreatment control values (*e.g.* Ref. 30). Such ratioing at least cancels out variable dye loading and pathlength if bleaching and cell shape change have not been significant. Of course $[Ca^{2+}]_i$ is calibrated not in absolute terms but only relative to the resting level, but that can often be measured independently or assumed to be spatially uniform and within a factor of two of 10^{-7} M. For many problems such accuracy may suffice.

A third mode of ratioing, first shown for quin-2 by Wages *et al.* (31), would rely on the different excited state lifetimes of the free *versus* Ca^{2+}-bound indicator. If the excited-state decay could be resolved into the exponential components corresponding to the two dye species, the ratio of the constituent amplitudes would reveal $[Ca^{2+}]_i$. Unfortunately the high extinction coefficients and modest quantum efficiencies of the present dyes suggest that the lifetimes are likely to be very short, 10^{-11} to 10^{-9} s for the free and bound indicator. With current technology, it would be impossible or at least very expensive to resolve such subnanosecond components within acquisition times of seconds or less in small tissue samples with limited dye concentrations. Spatially resolved imaging of such decay amplitude ratios would be yet harder.

Our testing has focused on the fluorescein rather than rhodamine analogs because the former have Ca^{2+} affinities more suitable for our biological interests and emission wavelengths closer to the optimum for the photodetectors in our laboratory. Also, the rhodamines have shown preliminary signs of compartmentalized loading. One would expect that the large negative membrane potential of mitochondria would tend to trap delocalized cations like the esters of the rhodamine analogs. Indicators of mitochondrial Ca^{2+} would have their own distinct usefulness. Fluo-3 is generally preferable over fluo-1 and fluo-2 because of its lesser sensitivity to pH and its larger fluorescence enhancement on binding Ca^{2+}, though if a particular cell type were to show severe leakage of dye into acidic compartments, the quenching of fluo-2 by low pH might prove advantageous.

Biological tests of fluo-3 in lymphocytes and fibroblasts are reported in the accompanying paper (28). Fluo-3, rhod-2, and their acetoxymethyl (AM) esters are now commercially available from Molecular Probes (P. O. Box 22010, Eugene, OR 97402), to whom requests for samples should be directed.

REFERENCES

1. Tsien, R. Y. (1983) *Annu. Rev. Biophys. Bioeng.* **12,** 91–116
2. Rink, T. J., and Pozzan, T. (1985) *Cell Calcium* **6,** 133–144
3. Grynkiewicz, G., Poenie, M., and Tsien, R. Y. (1985) *J. Biol. Chem.* **260,** 3440–3450
4. Cobbold, P. H., and Rink, T. J. (1987) *Biochem J.* **248,** 313–328
5. Tsien, R. Y. (1988) *Trends Neurosci.* **11,** 419–424
6. Tsien, R. Y. (1989) *Annu. Rev. Neurosci.* **12,** 227–253
7. Williams, D. A., and Fay, F. S. (1986) *Am. J. Physiol.* **250,** C779–C791
8. Tsien, R. Y., and Zucker, R. S. (1986) *Biophys. J.* **50,** 843–853
9. Gurney, A. M., Tsien, R. Y., and Lester, H. A. (1987) *Proc. Natl. Acad. Sci. U. S. A.* **84,** 3496–3500
10. Adams, S. R., Kao, J. P. Y., Grynkiewicz, G., Minta, A., and Tsien, R. Y. (1988) *J. Am. Chem. Soc.* **110,** 3212–3220
11. Kaplan, J. H., and Ellis-Davies, G. C. R. (1988) *Proc. Natl. Acad. Sci. U. S. A.* **85,** 6571–6575
12. Taylor, D. L., and Wang, Y.-L. (1980) *Nature* **284,** 405–410
13. Tsien, R. Y. (1980) *Biochemistry* **19,** 2396–2404
14. Drexhage, K. H. (1973) in *Dye Lasers* (Schaefer, F. P., ed) pp. 144–193, Springer Publishing Company, New York
15. Bridges, J. W. (1981) in *Standards in Fluorescence Spectrometry* (Miller, J. N., ed) pp. 68–78, Chapman & Hall, London
16. Weber, G., and Teale, F. W. J. (1957) *Faraday Soc. Trans.* **53,** 646–655
17. Martell, A. E., and Smith, R. M. (1974) *Critical Stability Constants*, Vol. I, pp. xi–xii, 139, 199, and 269, Plenum Publishing Corp., New York
18. von Braun, J., and Aust, E. (1913) *Ber. Dtsch. Chem. Ges.* **49,** 989–999
19. Ehrlich, P., and Benda, L. (1913) *Ber. Dtsch. Chem. Ges.* **46,** 1931–1943
20. Grover, P. K., Shah, G. D., and Shah, R. C. (1955) *J. Chem. Soc. (Lond.)* 3982–3985
21. Parham, W. E., and Bradsher, C. K. (1982) *Acc. Chem. Res.* **15,** 300–305
22. Kurduker, R., and Subba Rao, N. V. (1963) *Proc. Indian Acad. Sci. Sect. A* **57,** 280–287
23. Griffiths, J. (1976) *Colour and Constitution of Organic Molecules*, pp. 250–265, Academic Press, London
24. Martin, M. M., and Lindqvist, L. (1975) *J. Luminescence* **10,** 381–390
25. Arslan, P., Di Virgilio, F., Beltrame, M., Tsien, R. Y., and Pozzan, T. (1985) *J. Biol. Chem.* **260,** 2719–2727
26. Metcalfe, J. C., Hesketh, T. R., and Smith, G. A. (1985) *Cell Calcium* **6,** 183–195
27. White, J. G., Amos, W. B., and Fordham, M. (1987) *J. Cell Biol.* **105,** 41–48
28. Kao, J. P. Y., Harootunian, A. T., and Tsien, R. Y. (1989) *J. Biol. Chem.* **264,** 8179–8184
29. Giesow, M. J. (1984) *Exp. Cell Res.* **150,** 29–35
30. Smith, S. J., and Augustine, G. J. (1988) *Trends Neurosci.* **11,** 458–464
31. Wages, J., Jr., Packard, B., Edidin, M., and Brand, L. (1987) *Biophys. J.* **51,** 284 (abstr.)